Probing the $WW\gamma$ vertex in $e^{\pm}p \to \nu\gamma X$

U. Baur
Physics Department, Florida State University, Tallahassee, Florida 32306

M. A. Doncheski
Physics Department, University of Wisconsin, Madison, Wisconsin 53706
(Received 4 March 1992)

We study the prospects of testing the $WW\gamma$ vertex in $e^-p \to \nu\gamma X$ and $e^+p \to \nu\gamma X$ at the DESY ep collider HERA and the combination of the CERN e^+e^- collider LEP and Large Hadron Collider (LHC), LEP/LHC. Destructive interference effects between the standard model and the anomalous contributions to the amplitude severely limit the sensitivity of both processes to nonstandard $WW\gamma$ couplings. Sensitivity limits for the anomalous $WW\gamma$ couplings κ and λ at HERA and LEP/LHC are derived, taking into account experimental cuts and uncertainties, and the form factor behavior of nonstandard couplings. These limits are found to be significantly weaker than those which can be expected from other collider processes within the next few years. At HERA, they are comparable to bounds obtained from S-matrix unitarity.

PACS number(s): 13.60.Hb, 12.15.Ji, 13.40.Fn, 14.80.Er

One of the prime targets for experiments at present and future colliders is the measurement of the $WW\gamma$ and WWZ couplings. In the standard model (SM) of electroweak interactions, these couplings are unambiguously fixed by the non-Abelian nature of the SU(2)×U(1) gauge symmetry. In contrast with low-energy and high-precision experiments at the Z peak, collider experiments offer the possibility of a direct, and essentially model-independent, measurement of the three vector-boson vertices. In the past a number of different collider processes which are sensitive to anomalous $WW\gamma$ and WWZ couplings have been studied (see, e.g., Refs. [1–7]). Analyzing the reaction $p\bar{p} \to e^{\pm}\nu\gamma X$, the UA2 Collaboration recently reported the first direct measurement of the $WW\gamma$ vertex [8]. More precise information on anomalous $WW\gamma$ couplings can soon be expected from Fermilab Tevatron experiments, as well as from the DESY ep collider HERA.

At ep colliders such as HERA (30-GeV electrons/positrons on 820-GeV protons; $\sqrt{s}=314$ GeV, $\mathcal{L}=2\times10^{31}$ cm^{-2} s^{-1}) or the combined CERN e^+e^- collider LEP and Large Hadron Collider (LHC) (60-GeV electrons/positrons on 7.7-TeV protons; $\sqrt{s}=1.36$ TeV, $\mathcal{L}=2.8\times10^{32}$ cm^{-2} s^{-1} [9]) single-W-boson production via $ep \to eW^{\pm}X$ and radiative charged-current scattering $ep \to \nu\gamma X$ offer chances to test the $WW\gamma$ vertex. Single-W-boson production in ep collisions has been studied extensively in the past [4,5]. The process $e^-p \to \nu\gamma X$ has only recently been investigated in Refs. [10,11]. In this paper we present an independent calculation of the process $e^-p \to \nu\gamma X$, using the most general $WW\gamma$ vertex compatible with Lorentz and electromagnetic gauge invariance. We also extend the existing studies, investigating the reaction $e^+p \to \nu\gamma X$, and take into account the form-factor behavior of the nonstandard $WW\gamma$ couplings required by S-matrix unitarity [12,13].

The process $ep \to \nu\gamma X$ offers potential advantages over eW production in measuring the $WW\gamma$ vertex. At HERA and to a smaller degree at LEP/LHC, W production proceeds close to the kinematical threshold; furthermore, only the leptonic decays of the W boson can be identified. Both factors reduce the number of events which can be utilized in analyzing the structure of the $WW\gamma$ vertex in $ep \to eWX$. On the other hand, $ep \to \nu\gamma X$ is a pure charged-current process which is suppressed by the large mass of the exchanged W. It is thus not clear *a priori* whether $ep \to \nu\gamma X$ or $ep \to eWX$ will be more sensitive to anomalous $WW\gamma$ couplings.

There are four Feynman diagrams contributing to the reaction $e^{\pm}p \to \nu\gamma X$ at the parton level. The photon can be either radiated from the incoming lepton or quark line, from the outgoing quark line, or from the exchanged W boson. Using the spinor technique described in Ref. [14], we have calculated the matrix elements for $e^{\pm}q \to \nu\gamma q'$ for the most general $WW\gamma$ vertex compatible with Lorentz and electromagnetic gauge invariance. Since the exchanged W couples to essentially massless quarks, which effectively ensures that $\partial_\mu W^\mu=0$, the $WW\gamma$ vertex depends on four free parameters only and can conveniently be described by the effective Lagrangian [2,15]

$$\mathcal{L}_{WW\gamma}=-ie\left\{(W^\dagger_{\mu\nu}W^\mu A^\nu-W^\dagger_\mu A_\nu W^{\mu\nu})+\kappa W^\dagger_\mu W_\nu F^{\mu\nu}+\frac{\lambda}{M_W^2}W^\dagger_{\lambda\mu}W^\mu{}_\nu A^{\nu\lambda}+\tilde{\kappa}W^\dagger_\mu W_\nu \tilde{F}^{\mu\nu}+\frac{\tilde{\lambda}}{M_W^2}W^\dagger_{\lambda\mu}W^\mu{}_\nu \tilde{F}^{\nu\lambda}\right\}. \quad (1)$$

Here A^μ and W^μ are the photon and W^- fields, respectively, $W_{\mu\nu}=\partial_\mu W_\nu-\partial_\nu W_\mu$, $F_{\mu\nu}=\partial_\mu A_\nu-\partial_\nu A_\mu$, and $\tilde{F}_{\mu\nu}=\frac{1}{2}\epsilon_{\mu\nu\rho\sigma}F^{\rho\sigma}$. e is the charge of the proton and M_W the mass of the W boson.

The first term in Eq. (1) arises from the minimal cou-

pling of the photon to the $W^{\pm}$ fields and is completely fixed by the charge of the W boson for on-shell photons. The κ and λ terms are related to the magnetic dipole moment μ_W and the electric quadrupole moment Q_W of the W^+:

$$\mu_W=\frac{e}{2M_W}(1+\kappa+\lambda)\ ,\quad Q_W=-\frac{e}{M_W^2}(\kappa-\lambda)\ . \tag{2}$$

Within the SM, at tree level,

$$\kappa=1 \quad \text{and} \quad \lambda=0\ . \tag{3}$$

The CP-violating couplings $\tilde{\kappa}$ and $\tilde{\lambda}$, which both vanish at tree level in the SM, are constrained by the electric dipole moment of the neutron to be smaller than $\sim 10^{-3}$ [16] in magnitude. Subsequently, we shall therefore concentrate on the anomalous couplings κ and λ.

Tree-level unitarity restricts the $WW\gamma$ couplings to their (SM) gauge-theory values at asymptotically high energies [12,13]. This implies that any deviation $a=\Delta\kappa=\kappa-1$, λ from the SM expectation, has to be described by a form factor $a(q_W^2,\bar{q}_W^2,q_\gamma^2=0)$, which vanishes when either $|q_W^2|$, or $|\bar{q}_W^2|$, the absolute square of the four-momentum of the exchanged W bosons, becomes large. Consequently, we shall include form factors

$$a(q_W^2,\bar{q}_W^2,0)=a_0\left[\left(1-\frac{q_W^2}{\Lambda^2}\right)\left(1-\frac{\bar{q}_W^2}{\Lambda^2}\right)\right]^{-n}\ , \tag{4}$$

with $n=1$ in all our calculations. The scale Λ in Eq. (4) represents the scale at which new physics becomes important in the weak boson sector, e.g., as a result of a possible composite structure of the W boson. We shall use $\Lambda=1$ TeV in our numerical simulations.

We have compared our squared $e^-p\to\nu\gamma X$ matrix elements in the limit $\Lambda\to\infty$ with those of Ref. [11] for arbitrary values of κ and λ. The numerical agreement is excellent. Using the same set of parameters and cuts, we also agree with the cross-section values and the photon transverse-momentum distribution in the revised version of Ref. [10].

Subsequently, we shall discuss $e^-p\to\nu\gamma X$ and $e^+p\to\nu\gamma X$ in parallel. The SM parameters which will be used in all figures and tables are $M_W=80$ GeV and $\sin^2\theta_W=0.23$. The cross section for $e^{\pm}p\to\nu\gamma X$ is proportional to α^3, where α is the electromagnetic coupling constant. Since a real photon is emitted, one factor is evaluated at scale m_e^2, where m_e is the electron mass [$\alpha(m_e^2)=\frac{1}{137}$], and the two remaining factors are taken as $\alpha(M_W^2)=\frac{1}{128}$. For the proton structure functions, we use the Harriman-Martin-Roberts-Stirling set B [HMRS(B)] [17] with the scale Q^2 given by the four-momentum transfer to the scattered quark. Uncertainties in the energy measurements of the photon and jet in the detector are taken into account by Gaussian smearing of the four-momenta with standard deviation $\sigma=(0.15\ \text{GeV}^{1/2})\sqrt{E}$ and $(0.35\ \text{GeV}^{1/2})\sqrt{E}$, respectively.

The signal we are investigating consists of a photon, missing transverse momentum $\not{p}_T$ which originates from the neutrino, and a jet produced by the quark struck inside the proton. In order to regulate the infrared and collinear singularities present in $e^{\pm}p\to\nu\gamma X$, it is necessary to impose a nonzero cut on the photon transverse momentum $p_{T\gamma}$ and the jet photon separation $\Delta R_{j\gamma}=[(\Delta\phi_{j\gamma})^2+(\Delta\eta_{j\gamma})^2]^{1/2}$ in the pseudorapidity-azimuthal angle plane.

At HERA energies the $\gamma j\not{p}_T$ final state is predominantly produced from a valence u quark (d quark) in the proton for e^-p (e^+p) collisions. Photons in the collinear region therefore are radiated mostly from (final state) d (u) quarks in $e^-p\to\gamma j\not{p}_T$ ($e^+p\to\gamma j\not{p}_T$). Because of the larger electric charge of the u quarks, the collinear singularity is thus expected to be considerably more pronounced in the e^+p case. On the other hand, the difference in the u- and d-valence-quark distributions in the proton tends to suppress the $e^+p\to\gamma j\not{p}_T$ cross section.

Both effects are clearly reflected in the distributions of the jet photon separation $\Delta R_{j\gamma}$ and the invariant mass $m_{j\gamma}$, shown in Fig. 1. To simulate roughly the finite acceptance of detectors, we require $p_{T\gamma}>5$ GeV, a missing transverse momentum, and a jet p_T of $\not{p}_T$, $p_{T_j}>10$ GeV, and impose a photon and jet rapidity cut of $|\eta_\gamma|$, $|\eta_j|<3.5$. At large $\Delta R_{j\gamma}(m_{j\gamma})$, the rate for $e^+p\to\gamma j\not{p}_T$ is suppressed. In the collinear region, however, the $e^+p\to\gamma j\not{p}_T$ cross section rises much faster than the $e^-p\to\gamma j\not{p}_T$ rate, and the two cross sections are very similar. The peak at $\Delta R_{j\gamma}\approx\pi$ and $m_{j\gamma}\approx 30$ GeV arises from photons which are radiated from the incoming $e^{\pm}$ line. The $j\gamma$ invariant-mass distribution shows a rather long tail, extending out to about one-half of the available center-of-mass energy.

Because of the infrared singularity associated with photon emission from the incoming quark and lepton line, the transverse-momentum distribution of the photon strongly peaks at small $p_{T\gamma}$ values. Since the $WW\gamma$ vertex does not enter those diagrams, the signal at low $p_{T\gamma}$ is insensitive to anomalous $WW\gamma$ couplings, and no sensitivity is lost by requiring a hard photon with $p_{T\gamma}>10$ GeV (20 GeV) at HERA (LEP/LHC). The transverse-momentum distribution of the photon in $e^{\pm}p\to\gamma j\not{p}_T$ at HERA is shown in Fig. 2 for the SM (solid line) and anomalous values of κ and λ. Figure 3 displays $d\sigma/dp_{T\gamma}$ at LEP/LHC. We have imposed a jet and missing p_T cut of p_{Tj}, $\not{p}_T>10$ GeV (20 GeV) at HERA (LEP/LHC) and a jet pseudorapidity cut of $|\eta_j|<3.5$ (4.5). These cuts are representative for the typical angular coverage of detectors at HERA [18] and LEP/LHC [19]. Furthermore, we have required $|\eta_\gamma|<3.5$ and the jet and photon to be well separated, $\Delta R_{j\gamma}>0.5$.

From Figs. 2 and 3, it is obvious that $e^{\pm}p\to\gamma j\not{p}_T$ is sensitive to anomalous $WW\gamma$ couplings at large values of $p_{T\gamma}$. However, the Feynman diagram involving the $WW\gamma$ vertex contains two W propagators and thus is suppressed with respect to the bremsstrahlung diagrams. As a result, at HERA, rather large anomalous couplings are necessary to produce significant deviations from the SM $p_{T\gamma}$ distribution. Figures 2(b) and 3(b) show that the photon transverse-momentum distribution for $e^+p\to\gamma j\not{p}_T$ falls considerably faster than for $e^-p\to\gamma j\not{p}_T$ in the SM. Furthermore, for a given (nonstandard) value of

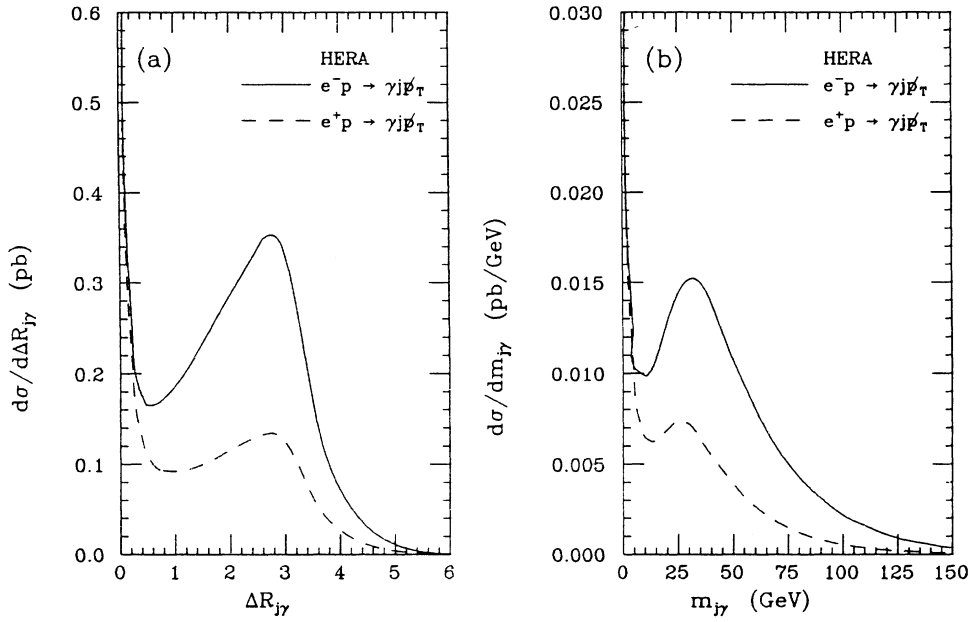

FIG. 1. Distribution of (a) the jet photon separation $\Delta R_{j\gamma}$ and (b) the jet photon invariant mass $m_{j\gamma}$ for $e^-p \to \gamma j \not{p}_T$ (solid line) and $e^+p \to \gamma j \not{p}_T$ (dashed line) at HERA in the SM. The cuts imposed are specified in the text.

κ or λ, deviations from the SM prediction are larger in $e^+p \to \gamma j \not{p}_T$. Whereas the form-factor behavior negligibly influences predictions for HERA, cross sections are reduced by about a factor 2 at LEP/LHC for anomalous $WW\gamma$ couplings and large photon transverse momenta.

At HERA as well as LEP/LHC energies, the sensitivity to anomalous couplings in $e^{\pm}p \to \gamma j \not{p}_T$ effectively stems from regions in phase space where the anomalous contributions to the cross section are smaller than the SM expectation. One therefore expects that interference effects between the SM amplitude and the anomalous contributions to the amplitude play a non-negligible role. This effect is most pronounced for anomalous values of κ. At intermediate photon transverse momenta, destructive

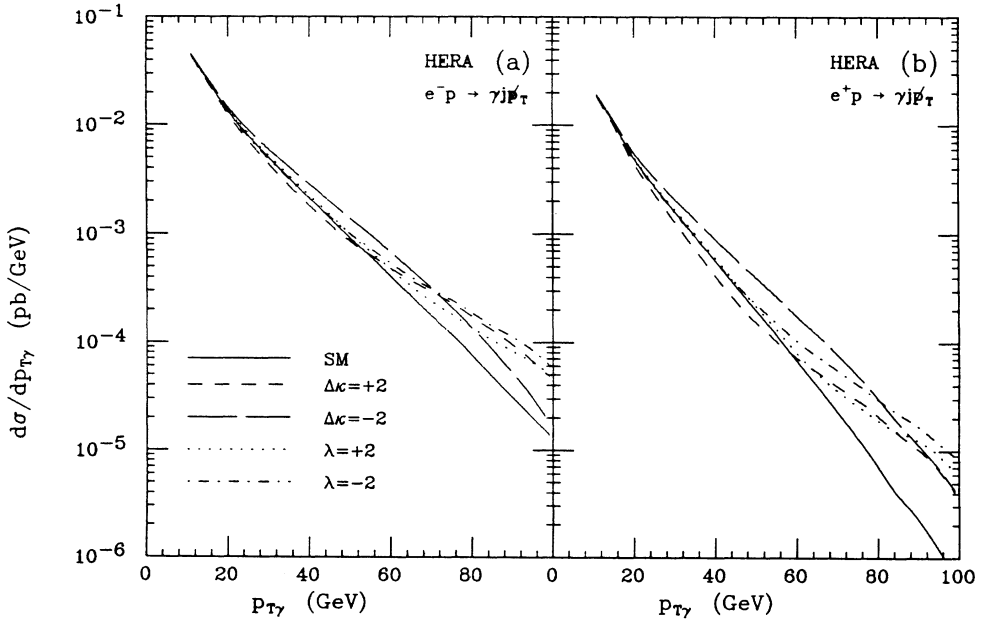

FIG. 2. Transverse-momentum distribution of the photon in (a) $e^-p \to \gamma j \not{p}_T$ and (b) $e^+p \to \gamma j \not{p}_T$ at HERA for the SM (solid line) and various anomalous values of κ and λ. Cuts are specified in the text.

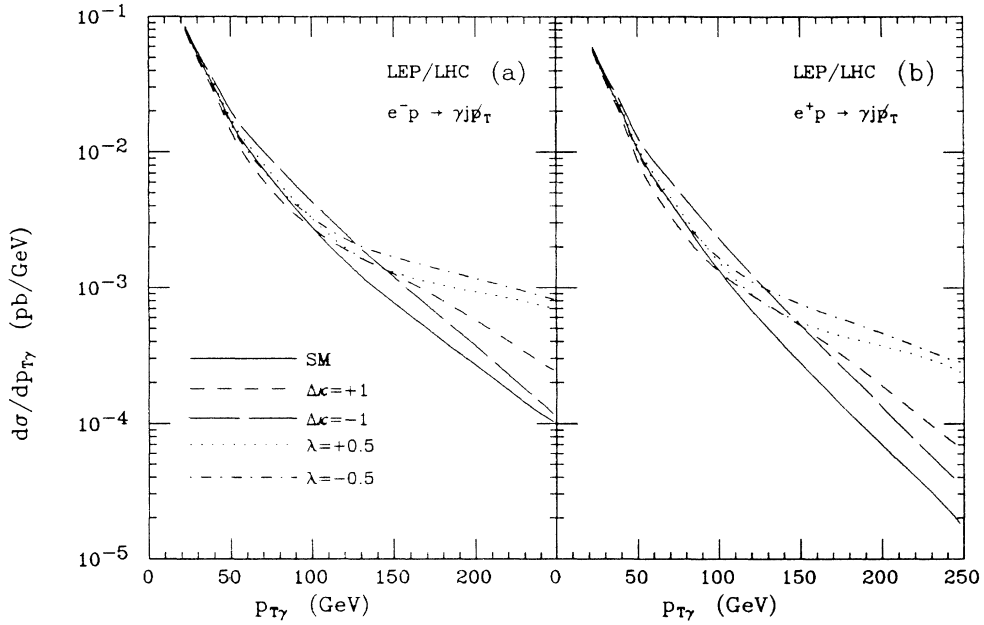

FIG. 3. Transverse-momentum distribution of the photon in (a) $e^-p \to \gamma j \not{p}_T$ and (b) $e^+p \to \gamma j \not{p}_T$ at LEP/LHC for the SM (solid line) and various anomalous values of κ and λ. Cuts are specified in the text.

interference causes $d\sigma/dp_{T\gamma}$ to dip below the SM prediction for positive values of $\Delta\kappa$. At large values of $p_{T\gamma}$, the interference term changes sign and significantly reduces the sensitivity to negative values of $\Delta\kappa$. In contrast with naive expectations, deviations from the SM prediction do not grow with increasing $p_{T\gamma}$ at HERA and LEP/LCH energies for $\Delta\kappa<0$ (provided that $|\Delta\kappa|$ is not too large).

This effect is enhanced, in particular in the e^-p case, by the finite rapidity cut imposed on the jet in Figs. 2 and 3. For large values of the photon transverse momentum and negative $\Delta\kappa$, the jet has a rapidity distribution which extends to considerably larger (negative) rapidities than for the SM or other anomalous $WW\gamma$ couplings. This is demonstrated in Fig. 4, where we show the jet pseudorapidity distribution for $e^-p \to \gamma j \not{p}_T$ at LEP/LHC in the region $p_{T\gamma}>200$ GeV in the SM case (solid line), for $\Delta\kappa=\pm 1$, and for $\lambda=0.1$. With the exception of η_j and $p_{T\gamma}$, all other cuts are as in Fig. 3. The incoming proton is assumed to move in the *negative* z direction. For $\Delta\kappa=-1$, the η_j distribution peaks at a somewhat larger value than in the other cases, and a substantial portion of the cross section originates from the region $\eta_j<-3.5$.

The η_j distribution directly reflects the properties of the anomalous contributions to the helicity amplitudes. For nonstandard values of κ, the photon mostly couples to longitudinally polarized W's at high energies [13]. The situation in $e^\pm p \to \gamma j \not{p}_T$ thus is similar to that of heavy-Higgs-boson production via vector-boson fusion at hadron colliders. Heavy Higgs bosons mostly couple to longitudinal vector bosons, which causes the jet rapidity distribution in $qq \to qqH$ to peak at large η_j [20]. Indeed, in the region $\eta_j \lesssim -4.5$ and at large $p_{T\gamma}$, the jet rapidity distributions for $\Delta\kappa=+1$ and -1 in $e^-p \to \gamma j \not{p}_T$ are very similar, indicating that the anomalous contribution dominates in this region. In the more central rapidity region, the largest contribution to the cross section originates from the interference term, which tends to cancel against

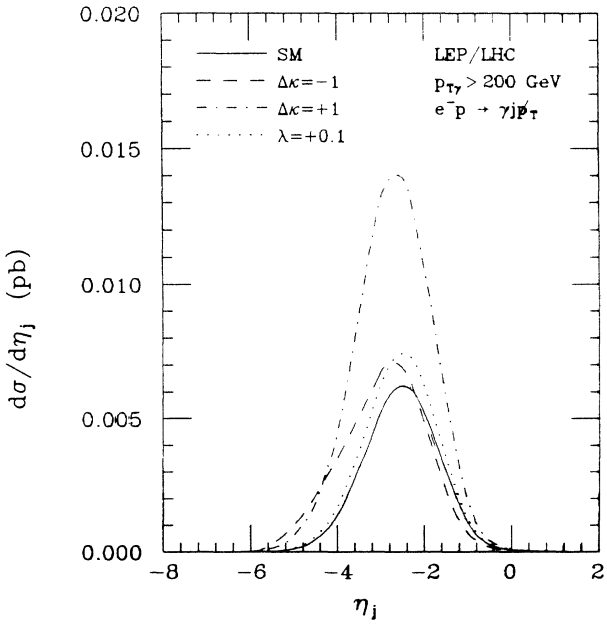

FIG. 4. Jet pseudorapidity distribution for $e^-p \to \gamma j \not{p}_T$ at LEP/LHC in the region $p_{T\gamma}>200$ GeV. The solid line displays the SM result, whereas the dashed, dot-dashed, and dotted curves show the predictions for $\Delta\kappa=-1$, $\Delta\kappa=+1$, and $\lambda=0.1$.

the SM contribution for negative $\Delta\kappa$.

As mentioned above, rather large anomalous couplings are necessary in order to produce measurable effects at HERA. This qualitative statement can be made more quantitative by deriving those values of κ and λ which would give rise to a deviation from the SM at the 90% and 69% confidence levels (C.L.'s) in the $p_{T\gamma}$ spectrum for an integrated luminosity of $\int \mathcal{L}\, dt = 10^3$ pb^{-1}, calculated within the cuts specified above. At HERA, an integrated luminosity of 1000 pb^{-1} corresponds to at least five years of running. The confidence level is calculated by splitting the $p_{T\gamma}$ distribution into six (ten) bins at HERA (LEP/LHC) for $e^-p \to \gamma j \not{p}_T$ and into four (eight) bins for $e^+p \to \gamma j \not{p}_T$. The last $p_{T\gamma}$ bin contains all events above a certain threshold, in order to achieve a sizable counting rate (more than five events) in each bin. This procedure guarantees that in our calculation a high confidence level cannot arise from a single event at high p_T, where the SM predicts, say, only 0.01 events. In order to derive realistic limits, we allow for a normalization uncertainty of the SM cross section of $\Delta\mathcal{N} = 30\%$. No attempt has been made to take into account the possible change in the shape of the $p_{T\gamma}$ distribution due to higher-order QCD corrections.

To illustrate the sensitivities which can be achieved, we list the minimal anomalous couplings, which would give rise to a 90% or 69% C.L. effect, in Table I for the case where only one coupling at a time is assumed to be different from the SM value. Although the effects of anomalous $WW\gamma$ couplings on the photon transverse-momentum distribution are more pronounced in $e^+p \to \gamma j \not{p}_T$, the smaller event rate, combined with the faster falling $p_{T\gamma}$ distribution, in general results in limits which are significantly weaker than those for $e^-p \to \gamma j \not{p}_T$ at HERA. Only for $\Delta\kappa < 0$ are the sensitivity limits for $e^+p \to \gamma j \not{p}_T$ and $e^-p \to \gamma j \not{p}_T$ comparable. Even at LEP/LHC the bounds for e^-p collisions are slightly better. The limits shown in Table I are somewhat weaker than those presented in Ref. [11], mostly as a result of the possible normalization uncertainty in the SM prediction which we included in our analysis. Because interference terms, i.e., terms linear in $\Delta\kappa$ and λ, dominate over those quadratic in the anomalous couplings, the bounds scale essentially with the square root of the integrated luminosity.

TABLE I. Sensitivities achievable at the 90% and 69% C.L. for the anomalous $WW\gamma$ couplings $\Delta\kappa = \kappa - 1$ and λ in $e^-p \to \gamma j \not{p}_T$ and $e^+p \to \gamma j \not{p}_T$ at HERA and LEP/LHC for an integrated luminosity of 1000 pb^{-1}. Only one coupling at a time is assumed to be different from the SM value.

Coupling	C.L.	HERA	LEP/LHC
		$e^-p \to \gamma j \not{p}_T$	
$\Delta\kappa$	90%	$+2.2$ -2.4	$+0.44$ -0.54
	69%	$+1.3$ -1.4	$+0.25$ -0.30
λ	90%	$+2.8$ -2.1	$+0.17$ -0.12
	69%	$+2.1$ -1.3	$+0.12$ -0.08
		$e^+p \to \gamma j \not{p}_T$	
$\Delta\kappa$	90%	$+4.0$ -2.2	$+0.53$ -0.53
	69%	$+3.0$ -1.1	$+0.31$ -0.30
λ	90%	$+4.8$ -3.8	$+0.21$ -0.16
	69%	$+3.1$ -2.3	$+0.16$ -0.10

Finally, we compare the limits achievable in $e^{\pm}p \to \gamma j \not{p}_T$ with bounds from S-matrix unitarity and the sensitivity to non-gauge-theory terms in the $WW\gamma$ vertex accessible in other present and future collider experiments. Bounds from S-matrix unitarity depend explicitly on the functional form and the scale Λ of the form factor. Varying only one coupling at a time, the following upper limits are obtained from unitarity for the form factor of Eq. (4) and $\Lambda \gg M_W$:

$$n=1: \begin{cases} |\Delta\kappa| \lesssim 1.9\ \text{TeV}^2/\Lambda^2 \\ |\lambda| \lesssim 1.0\ \text{TeV}^2/\Lambda^2 , \end{cases} \qquad n=2: \begin{cases} |\Delta\kappa| \lesssim 7.6\ \text{TeV}^2/\Lambda^2 \\ |\lambda| \lesssim 4.0\ \text{TeV}^2/\Lambda^2 . \end{cases} \tag{5}$$

Comparing the bounds listed in Table I with Eq. (5), one observes that measuring the anomalous $WW\gamma$ couplings in either $e^-p \to \gamma j \not{p}_T$ or $e^+p \to \gamma j \not{p}_T$ at HERA will not significantly improve the limits from S-matrix unitarity.

As we mentioned at the beginning, experiments at HERA, studying eW production, will also be able to probe the $WW\gamma$ vertex. For the same integrated luminosity used to derive the limits of Table I, the bounds achievable in $ep \to eWX$ [5] are about a factor 2–3 better than those from $e^{\pm}p \to \gamma j \not{p}_T$. Even at LEP/LHC, eW production will be somewhat more sensitive. The UA2 Collaboration has recently measured κ and λ in the process $p\bar{p} \to e^{\pm}\nu\gamma X$ at the CERN $p\bar{p}$ collider, obtaining [8]

$$\kappa = 1^{+2.6}_{-2.2} \text{ for } (\lambda = 0), \quad \lambda = 0^{+1.7}_{-1.8} \text{ (for } \kappa = 1) . \tag{6}$$

The errors in Eq. (6) are already within a factor of 2 of, or even better than, those which can be expected from $e^{\pm}p \to \gamma j \not{p}_T$ with 1000 pb^{-1} at HERA. Moreover, they are expected to be reduced considerably in the near future with new Tevatron data. With an integrated luminosity of 100 pb^{-1}, $|\Delta\kappa|$ can be constrained to be less than 0.7–1.0 (1.1–1.5) at 69% (90%) C.L. in $p\bar{p} \to W^{\pm}\gamma$, whereas $|\lambda|$ can be measured to $|\lambda| < 0.25$–0.30 (0.40–0.50) [21]. An even more precise determination of the anomalous $WW\gamma$ couplings will be possible in $e^+e^- \to W^+W^-$ at LEP II, where an accuracy of $|\Delta\kappa|, |\lambda| \approx 0.1$–$0.2$ is expected [2].

In summary, we have presented an independent calculation of the process $e^-p \to \nu\gamma X$, using the most general $WW\gamma$ vertex allowed by Lorentz and electromagnetic

gauge invariance. Our matrix elements fully agree with those of Ref. [11], and our numerical results are compatible with those presented in the revised version of Ref. [10]. We also explored the possibilities of probing the $WW\gamma$ vertex in the reaction $e^+p \to \nu\gamma X$. Although the effects of anomalous $WW\gamma$ couplings on the photon transverse-momentum distribution are more pronounced in $e^+p \to \gamma j\not{p}_T$, the smaller event rate, in particular at large photon transverse momenta, severely limits the bounds on $\Delta\kappa$ and λ which can be achieved. We found that they are, at best, comparable to those obtained in $e^-p \to \nu\gamma X$. In the energy domain of HERA and LEP/LHC, destructive interference effects between the SM and anomalous contributions to the amplitude, combined with effects induced by the finite jet pseudorapidity coverage of detectors, result in sensitivity bounds for $e^\pm p \to \nu\gamma X$, which are significantly weaker than those which can be expected from $ep \to eWX$, $p\bar{p} \to e^\pm \nu\gamma X$, and $e^+e^- \to W^+W^-$ within the next few years. At HERA, the limits which can be achieved for κ and λ in $e^\pm p \to \nu\gamma X$ are similar to the bounds resulting from S-matrix unitarity.

We would like to thank W. Buchmüller, W. Smith, D. Zeppenfeld, and P. Zerwas for useful discussions. We are also grateful to H. Spiesberger for useful correspondence and his assistance in comparing our results with those of Ref. [11]. This work was supported in part by the U.S. Department of Energy under Contract No. DE-AC02-76ER00881 and Contract No. DE-FG05-87ER40319, in part by the Texas National Research Laboratory Commission under Grant No. RGFY9173, and in part by the University of Wisconsin Research Committee with funds granted by the Wisconsin Alumni Research Foundation.

[1] K. O. Mikaelian, Phys. Rev. D **17**, 750 (1978); K. O. Mikaelian, M. A. Samuel, and D. Sahdev, Phys. Rev. Lett. **43**, 746 (1979); C. L. Bilchak, R. W. Brown, and J. D. Stroughair, Phys. Rev. D **29**, 375 (1984); J. Cortes, K. Hagiwara, and F. Herzog, Nucl. Phys. **B278**, 26 (1986); U. Baur and D. Zeppenfeld, *ibid.* **B308**, 127 (1988).

[2] K. Hagiwara *et al.*, Nucl. Phys. **B282**, 253 (1987); D. Zeppenfeld, Phys. Lett. B **183**, 380 (1987).

[3] S. Willenbrock and D. Zeppenfeld, Phys. Rev. D **37**, 1775 (1988); K. Hagiwara, J. Woodside, and D. Zeppenfeld, *ibid.* **41**, 2113 (1990).

[4] E. Gabrielli, Mod. Phys. Lett. A **1**, 465 (1986); M. Böhm and A. Rosado, Z. Phys. C **42**, 479 (1989).

[5] U. Baur and D. Zeppenfeld, Nucl. Phys. **B325**, 253 (1989).

[6] E. Yehudai, Phys. Rev. D **41**, 33 (1990); **44**, 3434 (1991); S. Y. Choi and F. Schrempp, Phys. Lett. B **272**, 149 (1991).

[7] E. N. Argyres *et al.*, Phys. Lett. B **280**, 324 (1992).

[8] UA2 Collaboration, J. Alitti *et al.*, Phys. Lett. B **277**, 194 (1992).

[9] The LHC Study Group, CERN Report No. 91-03, 1991 (unpublished).

[10] S. Godfrey, Report No. OCIP C 91-2 (unpublished).

[11] T. Helbig and H. Spiesberger, Nucl. Phys. **B373**, 73 (1992).

[12] J. M. Cornwall, D. N. Levin, and G. Tiktopoulos, Phys. Rev. Lett. **30**, 1268 (1973); Phys. Rev. D **10**, 1145 (1974); C. H. Llewellyn Smith, Phys. Lett. **46B**, 233 (1973); S. D. Joglekar, Ann. Phys. (N.Y.) **83**, 427 (1974).

[13] U. Baur and D. Zeppenfeld, Phys. Lett. B **201**, 383 (1988).

[14] K. Hagiwara and D. Zeppenfeld, Nucl. Phys. **B274**, 1 (1986).

[15] K. Gaemers and G. Gounaris, Z. Phys. C **1**, 259 (1979).

[16] W. J. Marciano and A. Queijeiro, Phys. Rev. D **33**, 3449 (1986); F. Boudjema, K. Hagiwara, C. Hamzaoui, and K. Numata, *ibid.* **43**, 2223 (1991).

[17] P. N. Harriman, A. D. Martin, R. G. Roberts, and W. J. Stirling, Phys. Rev. D **42**, 798 (1990).

[18] ZEUS Collaboration, report, 1986 (unpublished); status report, 1989 (unpublished).

[19] J. Feltesse, in *Proceedings of the ECFA Large Hadron Collider Workshop,* Aachen, Germany, 1990, edited by G. Jarlskog and D. Rein (CERN Report No. 90-10, CERN, Geneva, 1990), Vol. I, p. 219.

[20] R. N. Cahn, S. D. Ellis, R. Kleiss, and W. J. Stirling, Phys. Rev. D **35**, 1626 (1987); R. Kleiss and W. J. Stirling, Phys. Lett. B **200**, 193 (1988); U. Baur and E. W. N. Glover, Nucl. Phys. **B347**, 12 (1990); V. Barger *et al.*, Phys. Rev. D **44**, 2701 (1991).

[21] U. Baur and E. L. Berger, Phys. Rev. D **41**, 1476 (1990).